Journal of Biomolecular NMR, 6 (1995) 227–236
ESCOM

J-Bio NMR 304

The relationship between amide proton chemical shifts and secondary structure in proteins

Tetsuo Asakura[a,*], Kazuhiro Taoka[a], Makoto Demura[a] and Michael P. Williamson[b]

[a]*Department of Biotechnology, Tokyo University of Agriculture and Technology, Koganei, Tokyo 184, Japan*
[b]*Krebs Institute, Department of Molecular Biology and Biotechnology, University of Sheffield, Sheffield S10 2UH, U.K.*

Received 26 April 1995
Accepted 31 July 1995

Keywords: Chemical shift; Amide proton; Magnetic anisotropy; Secondary structure; Ribonuclease H; Leucine zipper

Summary

The parameters for HN chemical shift calculations of proteins have been determined using data from high-resolution crystal structures of 15 proteins. Employing these chemical shift calculations for HN protons, the observed secondary structure chemical shift trends of HN protons, i.e., upfield shifts on helix formation and downfield shifts on β-sheet formation, are discussed. Our calculations suggest that the main reason for the difference in NH chemical shifts in helices and sheets is not an effect from the directly hydrogen-bonded carbonyl, which gives rise to downfield shifts in both cases, but arises from an additional upfield shift predicted in helices and originating in residues i – 2 and i – 3. The calculations also explain the well-known relationship between amide proton shifts and hydrogen-bond lengths. In addition, the HN chemical shifts of the distorted amphipathic helices of the GCN4 leucine zipper are calculated and used to characterise the solution structure of the helices. By comparing the calculated and experimental shifts, it is shown that in general the agreement is good between residues 15 and 28. The most interesting observation is that in the N-terminal half of the zipper, although both calculated and experimental shifts show clear periodicity, they are no longer in phase. This suggests that for the N-terminal half, in the true average solution structure the period of the helix coil is longer by roughly one residue compared to the NMR structures.

Introduction

The chemical shift is the oldest and most fundamental NMR parameter, but unlike other parameters, such as NOEs or J-couplings, it has played little part in resonance assignments and/or NMR structure determination. However, chemical shifts are extremely sensitive to steric and electronic effects in general, and in particular to secondary and tertiary structure effects in proteins. The ranges of chemical shift changes resulting from structural effects and the accuracy of measurement significantly exceed those of other parameters, both in absolute and in relative terms. The reason why the chemical shift has played only a small role in NMR structural studies of proteins, in spite of these favourable features, appears to be the lack of an adequate theoretical treatment to account for the various contributions to the chemical shift (Szilágyi, 1995).

In our previous papers (Asakura et al., 1977a,b), we attempted to calculate the H^{α} chemical shift changes in poly-L-alanine from disordered to helical states by summations of chemical shift contributions from various sources, namely the effect of magnetic anisotropies of the C=O and C-N bonds, and the electric field effect (i.e., the polarisation of electrons along X-H bonds and the consequent change in shielding of the proton due to partially charged atoms), as well as the diamagnetic shielding contribution. The magnetic anisotropy effect is the major contributor to the conformation-dependent chemical shift, but is hard to evaluate accurately either theoretically or experimentally, using model compounds to provide a calibration (ApSimon et al., 1967; Zürcher, 1967). Since the number of proteins for which both chemical shift data and structural coordinates by X-ray and/or NMR methods are known is rapidly increasing, it is now possible to determine the parameters used in chemical shift calcula-

*To whom correspondence should be addressed.

tions from protein data directly. This results in an empirically determined set of parameters. A number of different types of parameter have been proposed recently, for example based on bond magnetic anisotropies (Williamson and Asakura, 1991,1993; Williamson et al., 1992), atomic anisotropies (Asakura et al., 1992a), or peptide group anisotropy (Ösapay and Case, 1991,1994). It is important that the appropriate set be chosen, both to allow a comparison with theoretical and model values, and in order to be able to interpret chemical shift changes in terms of meaningful local structural changes. Recently, we optimized the parameters for a number of models that have been proposed for calculating chemical shifts in proteins and peptides using experimental data on H^{α} shifts for a range of proteins with well-defined crystal structures (Williamson and Asakura, 1991,1993; Asakura et al., 1992a; Williamson et al., 1992). Several applications of the calculation have been proposed, particularly as an independent means of measuring the quality of a structure (either in the crystal or in solution), and in identifying possible assignment errors (Williamson and Asakura, 1992; Kikuchi et al., 1994; Williamson et al., 1995).

Other groups have conducted similar studies. Ösapay and Case (1991,1994) carried out an empirical analysis of proton chemical shifts from 17 proteins whose X-ray crystal structures had been determined and showed that a significant improvement over ring current theories can be made by including the effects of the magnetic anisotropy of the peptide group and estimates of backbone electrostatic contributions. In addition, they reported calculations on oligopeptide models for helices, sheets and turns to show how secondary structure affects backbone chemical shifts (Case et al., 1994; Ösapay and Case, 1994). Herranz et al. (1992) attempted to account for both H^{α} and HN conformational shifts simultaneously by proposing a two-term empirical expression for the effect of the peptide group. The choice of functional form for these two terms was based not so much on theoretical grounds, but rather had an empirical basis, with the objective of explaining experimental results or relationships, namely that the NH proton close to and on top of a peptide group plane experiences the largest observed upfield conformation shift, the H^{α} and HN protons of residues in β-sheet regions experience downfield shifts, whereas those in α-helix regions experience upfield shifts (Markley et al., 1967; Clayden and Williams, 1982; Dalgarno et al., 1983; Szilágyi and Jardetzky, 1989; Williamson, 1990; Wishart et al., 1991), and the existence of a quantitative relationship between HN proton chemical shifts and hydrogen-bond lengths for hydrogen-bonded groups in proteins (Wagner et al., 1983; Wishart et al., 1991).

In a previous paper (Asakura, 1981), the HN chemical shifts of 16-residue alanine oligopeptides with extended, α-helical and β-sheet structures were calculated theoretically through summation of the shielding contributions, in order to obtain insight into the contribution of peptide groups other than the nearest neighbors. For example, the upfield shift of NH protons located in the peptide plane has been predicted by such a chemical shift calculation and this was found to be very important in interpreting chemical shifts in α-helices. However, in this previous study the parameters for the proton chemical shift calculation were determined from the chemical shift values of simple amide compounds because of limited experimental data (Asakura et al., 1977a). When we used the value of the C=O bond anisotropy reported by Zürcher (1967), the HN chemical shifts of BPTI were reproduced well and could be used for the refinement of the side-chain conformation (Asakura et al., 1991,1992b).

In this paper, we report the determination of the parameters for HN chemical shift calculations of proteins using data from high-resolution crystal structures of 15 proteins. It is important to use high-quality structural information, because the HN chemical shift is strongly determined by the shielding contribution of its directly hydrogen-bonded carbonyl group, and is therefore very dependent on the accuracy of its coordinates. Using these chemical shift calculations for HN protons, the observed secondary structure chemical shift trends of HN protons, i.e., upfield shifts on helix formation and downfield shifts on β-sheet formation, can be discussed, especially with respect to the origin of the chemical shifts. Recently, the influence of distortions of amphipathic helices on HN chemical shifts has been discussed by various groups with regard to the quantitative relationship between chemical shifts and hydrogen-bond lengths for hydrogen-bonded groups (Bruix et al., 1990; Kuntz et al., 1991; Blanco et al., 1992; Jiménez et al., 1992; Zhou et al., 1992). Therefore, we discuss the relationship between our model and the previously used hydrogen-bond length dependence, and calculate the HN chemical shifts of the distorted amphipathic helices of the GCN4 leucine zipper (Oas et al., 1990; O'Shea et al., 1991; Saudek et al., 1991), using the calculations to characterise the structure of the helices.

Methods

The HN chemical shift is considered as a sum of several shielding effects, and can be expressed as follows (Williamson and Asakura, 1993):

$$\sigma^{obs} - \sigma^{random\ coil} = \sigma^{ring} + \sigma^{ani} + \sigma^{E}$$

where σ^{obs} is the observed HN chemical shift, $\sigma^{random\ coil}$ the random coil HN chemical shift reported by Wüthrich (1986), σ^{ring} the ring current shift, σ^{ani} the magnetic anisotropy effect from the carbonyl and C-N bonds of amide groups, and σ^{E} the electric field effect. Each shielding effect can be calculated according to the methods report-

ed previously (Williamson and Asakura, 1993) on the basis of the coordinates of the specified NH proton and other relevant atoms. σ^{ring} can be assumed to be independent of the other effects and is calculated using the Haigh–Mallion model (Haigh and Mallion, 1980), which was previously used for ring current effect calculations of H^{α} protons.

The equation for the HN chemical shift calculation can be recast as follows:

$$\sigma^{obs} - \sigma^{random\ coil} - \sigma^{ring} = \sigma^{ani\ C=O} + \sigma^{ani\ C-N} + \sigma^{E}$$
$$= (1/3r_{CO}^3)[\Delta\chi_{1CO}(1 - 3\cos^2\theta_{CO}) + \Delta\chi_{2CO}(1 - 3\cos^2\phi_{CO})]$$
$$+ (1/3r_{CN}^3)[\Delta\chi_{1CN}(1 - 3\cos^2\theta_{CN}) + \Delta\chi_{2CN}(1 - 3\cos^2\phi_{CN})]$$
$$+ \varepsilon_1 \sum(Q_i / r_i^2)\cos\theta_i$$

Here, the magnetic anisotropies of the C=O bond, $\Delta\chi_{1CO}$ and $\Delta\chi_{2CO}$, and those of the C-N bond, $\Delta\chi_{1CN}$ and $\Delta\chi_{2CN}$, as well as the coefficient ε_1 in the σ^E term are optimized by assessing the quality of the fit of observed to calculated HN chemical shift data of proteins. The definition of the other terms has been given by Williamson and Asakura (1993).

The criteria used for goodness of fit were the regression coefficient R and the standard deviation SD of the secondary shift, $\sigma^{obs*} = \sigma^{obs} - \sigma^{random\ coil}$, against the calculated value. In principle, the SD should be the better measure, since it measures the difference between calculated and experimental shifts directly, but both criteria were used to avoid falling into local minima during the refinement. The criteria used to select the proteins that were used in the database were that the protein should be almost completely assigned, should have been shown to have very similar structures in solution and in the crystal, and its crystal structure should have been determined at high resolution. The 15 proteins used which satisfy these conditions are: human lysozyme (Redfield and Dobson, 1990), hen egg white lysozyme (Redfield and Dobson, 1988), bacteriophage T4 lysozyme (McIntosh et al., 1990), bovine pancreatic ribonuclease A (Robertson et al., 1989), ribonuclease H (Yamazaki et al., 1993), human ubiquitin (DiStefano and Wand, 1987), streptococcal protein G B2-domain (Orban et al., 1992), bovine pancreatic trypsin inhibitor (BPTI) (Wagner et al., 1987), FK506-binding protein (Xu et al., 1993), glucose permease IIA (Fairbrother et al., 1992), III^{Glc} (Pelton et al., 1991), tendamistat (Kline and Wüthrich, 1986), Alzheimer's β-amyloid precursor protein (Heald et al., 1991), apo-neocarzinostatin (Adjadj et al., 1990), and ColE1 rop protein (Eberle et al., 1990). The Brookhaven Databank names are given in Table 1 (Bernstein et al., 1977; Abola et al., 1987). The resolution of the crystal structures of these proteins ranges from 1.0 Å for BPTI to 2.1 Å for III^{Glc}.

As noted above, the chemical shift of an amide proton depends strongly on the position of any hydrogen-bonded partners. Many amide protons, particularly those on the protein surface, are hydrogen bonded to water molecules, for which in many cases the coordinates are uncertain. For many amide groups on the protein surface there is no apparent hydrogen-bond partner in the crystal structure, although detailed studies suggest that almost all amide groups are in fact hydrogen bonded (Baker and Hubbard, 1984). When an amide proton is hydrogen bonded both to a protein functional group and to water, the hydrogen bond to water is usually the weaker bond and is therefore expected to have a lesser effect on the amide chemical shift. Therefore, in this study we have considered only those amide protons that are hydrogen bonded to protein functional groups, and we have not attempted detailed calculations for those that are hydrogen bonded to water or have no apparent hydrogen-bonding partners. The method of Kabsch and Sander (1983) was used to detect the presence of hydrogen bonds. We did not include amide chemical shift data for bifurcated hydrogen bonds in the chemical shift parameter determination. The number of hydrogen-bonded HN protons detected in our data set is 981 (out of a total of 1509 HN chemical shifts reported for these 15 proteins), which is sufficient for a statistically valid determination of the parameters.

The solvent-accessible area of amide protons was calculated using a CCP4 subroutine (Bailey, 1994) based on the algorithm of Lee and Richards (1971), using a radius of 1.4 Å for the water molecule. Calculation of HN chemical shifts requires the addition of HN protons to the heavy atoms in the crystal structure. In this work, the

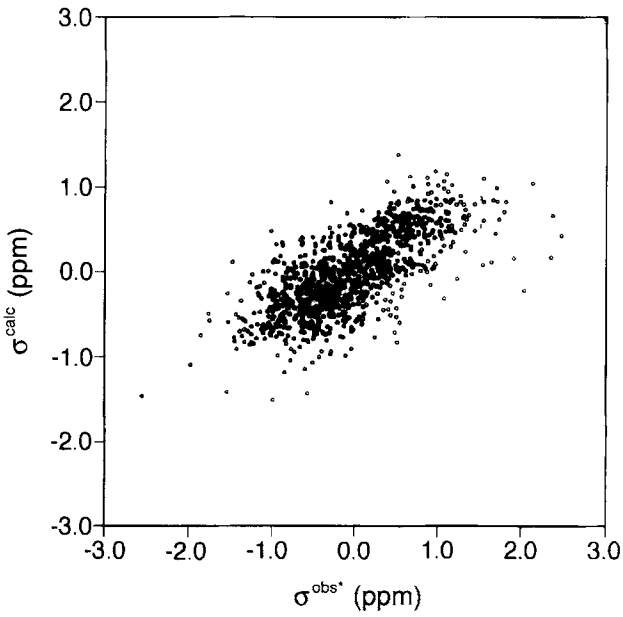

Fig. 1. Comparison of calculated (σ^{calc}) and observed ($\sigma^{obs*} = \sigma^{obs} - \sigma^{random\ coil}$) amide proton shifts, expressed as differences from the random coil values. The values for 981 hydrogen-bonded amide protons in 15 proteins are plotted. Positive and negative values indicate downfield and upfield shifts, respectively. The SD and R values are 0.492 and 0.715, respectively.

protons were added with standard geometries, using an N-H bond length of 0.98 Å. The chemical shift calculation programs were written in Fortran and run on a Silicon Graphics personal Iris workstation, and are available through anonymous ftp from directory pub/uni/academic/I-M/mbb in ftp.shef.ac.uk. The simultaneous optimization of the chemical shift parameters, i.e., the magnetic anisotropies of the C=O bond, $\Delta\chi_{1CO}$ and $\Delta\chi_{2CO}$, and those of the C-N bond, $\Delta\chi_{1CN}$ and $\Delta\chi_{2CN}$, as well as the coefficient ε_1 in the σ^E term, was performed using Microsoft EXCEL.

Results and Discussion

Parameter determination for HN chemical shift calculation

The optimized values of the parameters (in $cm^3 \times 10^{-30}$) were −11 and −5 for the magnetic anisotropies of the C=O bond, $\Delta\chi_{1CO}$ and $\Delta\chi_{2CO}$, respectively, and −7 and +1 for those of the C-N bond, $\Delta\chi_{1CN}$ and $\Delta\chi_{2CN}$, respectively. The coefficient of the electric field effect was only 0.06 (compared to the optimized value for C-H shifts of 0.6). Therefore, the electric field effect was neglected in subsequent calculations. The SD and R were 0.492 and 0.715, respectively, for the 981 H-bonded NH protons shown in Fig. 1. The parameters obtained here were close to those determined from the α-proton chemical shift data set (−13 and −4 for the magnetic anisotropies of the C=O bond, and −11 and +1.4 for those of the C-N bond). The agreement of the parameters obtained independently using the NH and H^α data sets strongly confirms the validity of the parameters. When we used these parameters for all 1509 NH protons, as shown in Fig. 2, the fit was somewhat worse: SD = 0.535 and R = 0.667. The SD and R values for each protein are listed in Table 1. When the parameters obtained previously from α-protons (Williamson and Asakura, 1993) are used, the values obtained are SD = 0.530, R = 0.699 for H-bonded NH and SD = 0.556, R = 0.657 for all NH protons. Thus, these new parameters perform better in the HN chemical shift calculations, although the improvement in SD and R is small. Similar comparisons have been made by two other groups (Table 2). The results from all three groups are broadly comparable; they all have more difficulty in calculating amide protons than other protons, for reasons discussed below. These difficulties obscure any possible real differences between the different methods.

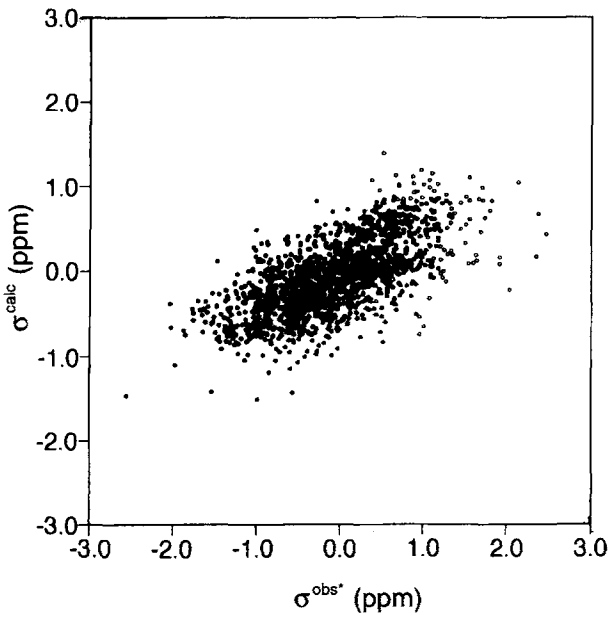

Fig. 2. Comparison of calculated (σ^{calc}) and observed ($\sigma^{obs*} = \sigma^{obs} - \sigma^{random\ coil}$) amide proton shifts, expressed as differences from the random coil values. The values for all 1509 amide protons in 15 proteins are plotted. The SD and R values are 0.535 and 0.667, respectively.

TABLE 1
SUMMARY OF FITS OF AMIDE PROTON SHIFTS

Protein name	PDB abbreviation	SD	R
Lysozyme (hen)	132L	0.522	0.588
β-amyloid protein	1AAP	0.593	0.825
III^{Glc}	1F3G	0.577	0.609
FK506-binding protein	1FKF	0.658	0.601
Glucose permease IIA	1GPR	0.564	0.652
Tendamistat	1HOE	0.472	0.683
Lysozyme (human)	1LZ1	0.541	0.566
Apo-neocarzinostatin	1NOA	0.465	0.636
Protein G	1PGX	0.487	0.737
ColE1 rop protein	1ROP	0.399	0.656
Ubiquitin	1UBQ	0.483	0.684
Ribonuclease H	2RN2	0.462	0.744
Lysozyme (T4)	3LZM	0.506	0.608
Ribonuclease A	3RN3	0.495	0.718
BPTI	5PTI	0.606	0.869

The results are calculated for the comparison of secondary shift ($\sigma^{obs} - \sigma^{random\ coil}$) with the value calculated by $\sigma^{ring} - \sigma^{ani}$ over all amide protons.

There could be various reasons for the discrepancies between the calculated and observed chemical shifts. One is the issue of chemical shift referencing, which is equally important for α-proton and HN chemical shifts (Wishart and Sykes, 1994; Szilágyi, 1995; Wishart et al., 1995). A more serious problem is the different experimental conditions used for each protein, such as temperature, concentration and pH, since the HN chemical shift is very sensitive to these factors. Another serious problem is the question which values should be used for the random coil HN shifts. Wishart et al. (1995) recently pointed out that the values of Bundi and Wüthrich (1979) are consistently higher (average 8.35 ppm versus 8.26 ppm) and substantially more dispersive (8.09–8.75 ppm versus 8.00–8.43 ppm) than their own data, which were obtained using a protected linear hexapeptide Gly-Gly-X-Ala-Gly-Gly (where X is any of the 20 common amino acids). Some amide chemical shifts are significantly different, particularly those for asparagine (8.75 ppm versus 8.40 ppm),

valine (8.44 ppm versus 8.03 ppm) and leucine (8.42 ppm versus 8.16 ppm). Wishart et al. (1995) considered the difference to be primarily the result of 'end group' and 'residual structure' effects, arising from Bundi and Wüthrich's use of unprotected tetrapeptides in high (50 mM) concentration without the presence of a denaturant.

A major reason for the discrepancies between calculated and observed HN shifts is the solvent effect, which is likely to be much more significant for HN than for α-protons. A qualitative picture of the importance of solvent effects is obtained by looking for a correlation between the difference $\sigma^{calc} - \sigma^{obs*}$, i.e., calculated minus experimental shift, and solvent exposure, as shown in Fig. 3. When HN protons are buried (solvent-accessible HN area < 2.5 Å^2), the distribution is approximately normal and the center is at $\sigma^{calc} - \sigma^{obs*} = 0$ ppm. However, when HN protons are relatively external (HN area ≥ 2.5 Å^2), the center of the distribution deviates from $\sigma^{calc} - \sigma^{obs*} = 0$ ppm to ca. −0.4 ppm. One reason for this change is undoubtedly the fact that the external amides are hydrogen bonded to 'invisible' water molecules, which are not included in the calculations.

Linear regression analysis of HN chemical shifts and hydrogen-bond length

Wagner et al. (1983) reported a correlation between secondary structure shifts and the inverse third power of distances d_N between HN protons of BPTI and nearby oxygen atoms:

$$\sigma^{obs*} - \sigma^{ring} = 19.2\ d_N^{-3} - 2.3 \text{ ppm}$$

Later studies by Wishart et al. (1991) proposed a simple inverse rather than an inverse cube distance dependence:

$$\sigma^{obs*} = 19\ d_N^{-1} - 9.7 \text{ ppm}$$

Therefore, the HN chemical shifts for the 981 hydrogen-bonded NH protons, corrected for ring current shifts, were plotted against the hydrogen-bond distance, as shown in Fig. 4.

The results reported in the previous section show that amide proton chemical shifts can be calculated well using

TABLE 2
COMPARISON OF DIFFERENT METHODS FOR CALCULATION OF AMIDE SHIFTS

Method	R	SD
Herranz et al. (1992)[a]	0.713	0.503
Ösapay and Case (1991)[b]	0.575 (0.721)	0.621 (0.506)
This work[a]	0.740	0.515

[a] Mean value for all amide protons of ubiquitin, ribonuclease A and BPTI.
[b] Mean value for all amide protons from 20 proteins.
Values between parentheses are for hydrogen-bonded amide protons.

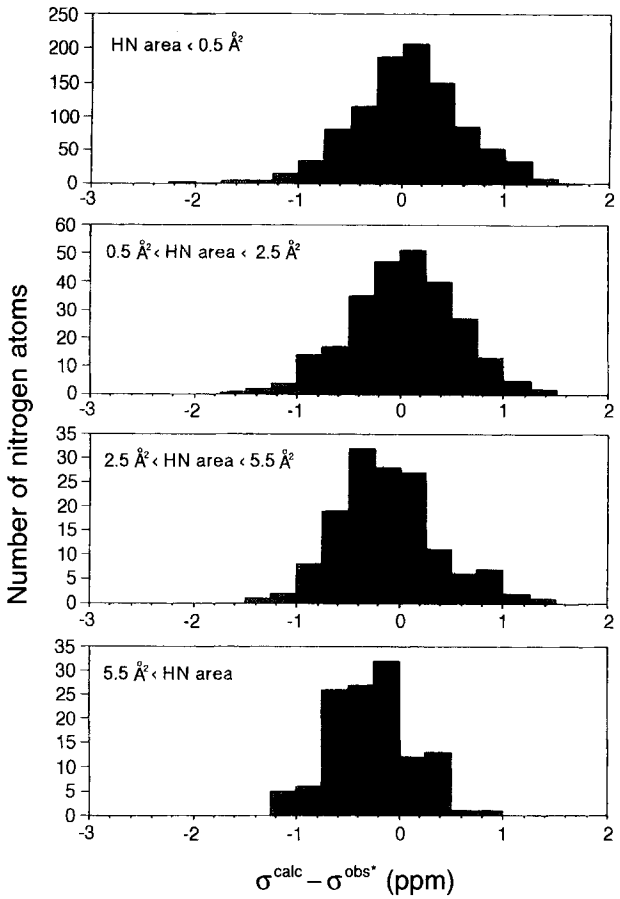

Fig. 3. Histograms representing the distribution of surface exposure of nitrogen atoms (with radius extended to allow for NH) against the difference $\sigma^{obs*} = \sigma^{obs} - \sigma^{random\ coil}$, i.e., calculated minus observed shift, using the same set of 1509 amide protons as described in the legend to Fig. 2.

the magnetic anisotropy of the carbonyl group as the dominant term. This expression already contains a d_N^{-3} term, similar to that calculated by Wagner et al. (1983). The differences between the magnetic anisotropy term and a straight d_N^{-3} term are that the former contains an angular dependence (which has a relatively small effect here, because the geometry of hydrogen bonds is fairly constant), and also that the distance d_N used by Wagner et al. is the H-O distance, whereas the distance used in the magnetic anisotropy calculation is to the center of anisotropy of the C=O bond and is thus about 0.12 Å longer. The net effect of these differences is to weaken the total d^{-3} dependence. It is therefore expected that both a d_N^{-3} term and a d_N^{-1} term should give a reasonably good fit to the observed chemical shifts. For d_N^{-3}, the correlation was as follows:

$$\sigma^{obs*} - \sigma^{ring} = 10.05\ d_N^{-3} - 1.25 \quad (SD = 0.590,\ R = 0.572)$$

and for d_N^{-1}:

$$\sigma^{obs*} - \sigma^{ring} = 8.29\ d_N^{-1} - 4.11 \quad (SD = 0.575,\ R = 0.604)$$

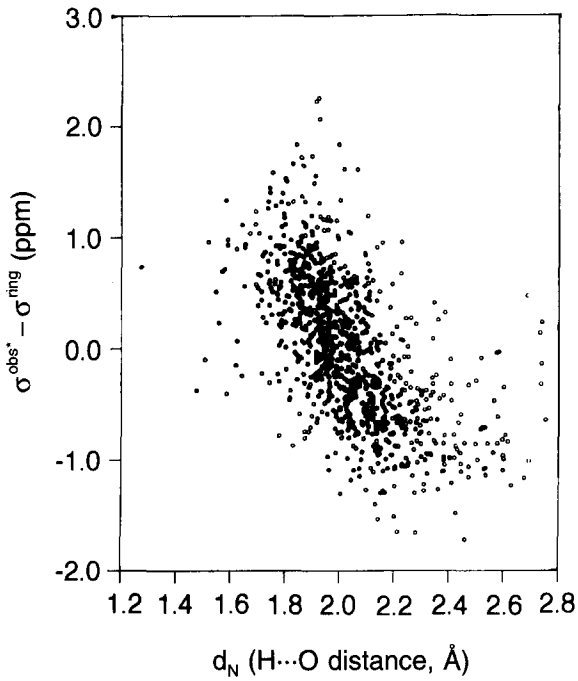

Fig. 4. Plot of the observed ($\sigma^{obs*} - \sigma^{ring}$) amide proton shifts, expressed as differences from the sum of random coil values and ring current shifts for hydrogen-bonded amide protons in 15 proteins versus the distance of these protons from the hydrogen-bonded oxygen atom, d_N.

As expected, the correlations obtained in the previous section are better than those obtained by this simple distance dependence, because of the additional terms included, such as peptide C-N bond anisotropy.

Dependence of HN chemical shifts on secondary structure

Upfield HN shifts on helix formation and downfield shifts on β-sheet formation have been reported by several authors (Markley et al., 1967; Clayden and Williams, 1982; Dalgarno et al., 1983; Szilágyi and Jardetzky, 1989; Williamson, 1990; Wishart et al., 1991). We have previously studied the structural origins of similar effects on H^{α} shifts (Williamson et al., 1992). In order to examine the typical contribution of the C=O and C-N bond anisotropies of amide groups to the chemical shift of HN protons in the center of an α-helix, HN chemical shifts were calculated for the protons in a model helix, namely an α-helical alanine oligopeptide, $-(Ala)_{16}-$, where the ϕ and φ values of each residue were assumed to be −65° and −39°, respectively (Laskowski et al., 1993). The largest contribution (0.24 ppm downfield) to the chemical shift of the HN of residue i (HN_i) comes from the C=O bond anisotropy of its hydrogen-bonded partner, residue i−4. However, less expected contributions to the chemical shift of HN_i come from $C{=}O_{i-3}$ (0.31 ppm upfield) and from $C\text{-}N_{i-2}$ (0.30 ppm upfield). (Note that $C\text{-}N_{i-2}$ refers to the magnetic anisotropy caused by the peptide C-N bond between the C' of residue i−2 and the N of residue i−1.) Thus, the HN proton in alanine residue i is located in the shielding (upfield shift) region of the C=O bond anisotropy of the (i−3)th alanine and of the peptide C-N bond anisotropy of the (i−2)th alanine residue, and it is these upfield effects that counteract the downfield effect caused by the directly bonded carbonyl and produce the net observed upfield shift. Herranz et al. (1992) used calculated data from ubiquitin to emphasize the observation that protein NH protons on top of the plane of the preceding peptide group experience large upfield shifts, which are similar to the well-known upfield aromatic ring current shift, in agreement with our previous predictions

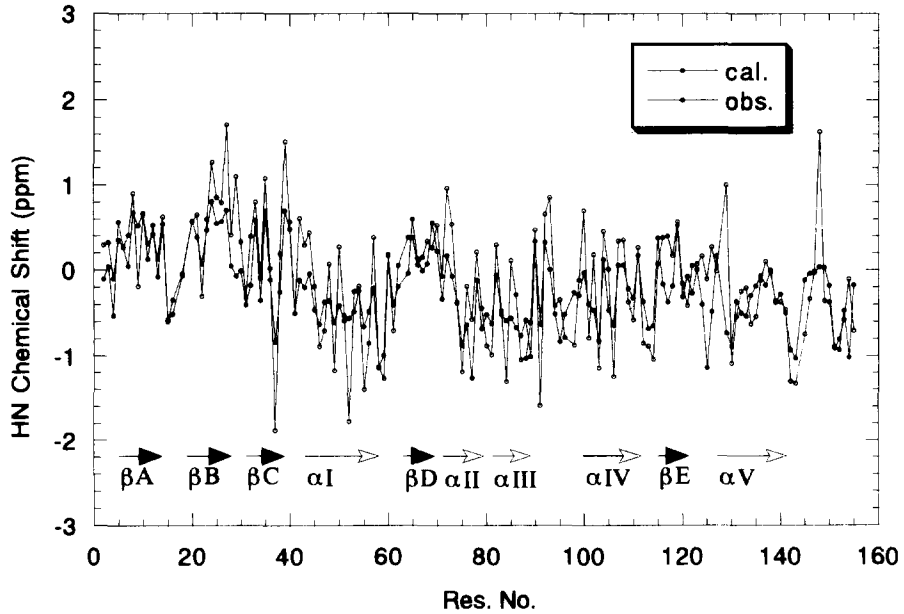

Fig. 5. Plot of sequence dependence of the calculated (●) and observed (○) amide proton shifts, expressed as differences from the random coil values, for all amide protons in ribonuclease H. The SD and R values are 0.462 and 0.774, respectively. The helix and sheet regions are also shown.

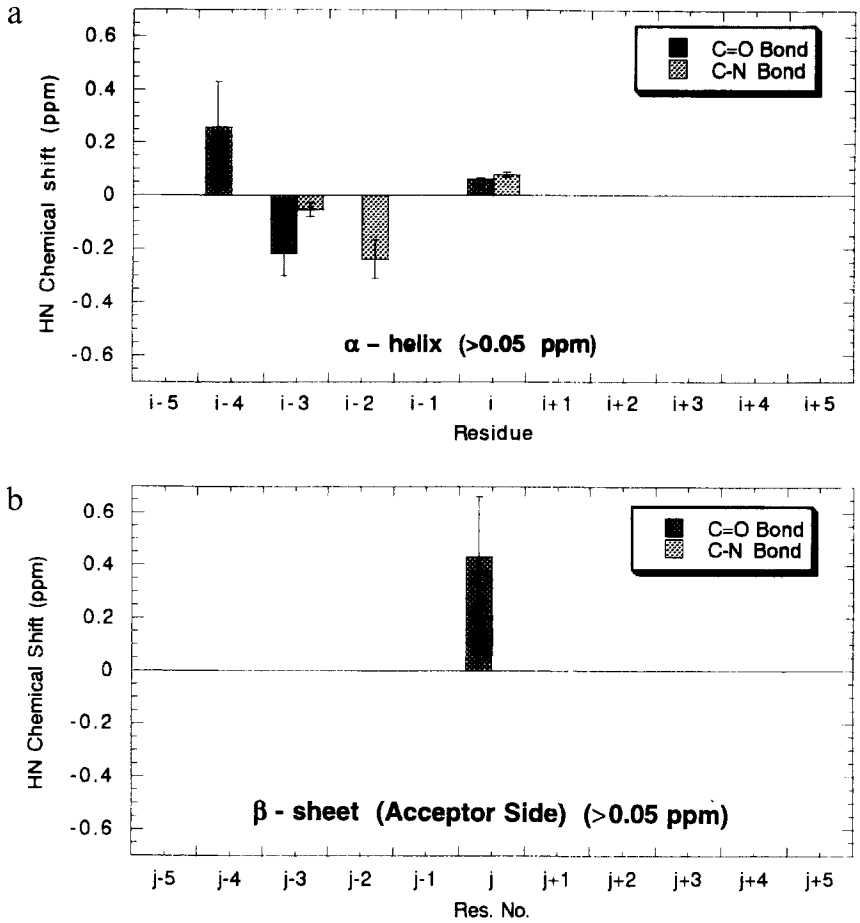

Fig. 6. (a) Histograms representing the calculated magnetic anisotropy contributions to the *i*th amide proton chemical shift within helical regions in ribonuclease H. The averaged values and their standard deviations were calculated using the hydrogen-bonded HN protons in helical regions (see text). The contributions are divided into bond magnetic anisotropy effects from the C=O and C-N bonds. (b) Histogram representing the calculated magnetic anisotropy contributions to the *i*th amide proton chemical shift within β-sheet regions of ribonuclease H. The residue to which residue i is hydrogen bonded is denoted j. The contribution from C=O and C-N anisotropy of residue i−1 is independent of the conformation and is not included in the plot.

(Asakura, 1981). The calculations reported here show that this 'out of plane' effect is largely due to bond magnetic anisotropy.

In order to check this tendency in real cases, chemical shift contributions were examined in detail for ribonuclease H (Katayanagi et al., 1992; Yamazaki et al., 1993). The plot of the calculated and observed HN chemical shifts against the residue number is shown in Fig. 5, which also shows the regions of α-helix and β-sheet. The SD and R were 0.462 and 0.744, respectively. The observed data tend to have a larger magnitude than the calculated data, but generally the agreement between calculated and observed shifts is reasonable. The averaged values and their standard deviations are shown in Fig. 6a, calculated using 41 HN protons in helical regions, made up of all 62 protons in helices except for the HN protons that do not take part in regular α-helical hydrogen bonding according to the Kabsch and Sander (1983) algorithm. Only contributions of more than 0.05 ppm are taken into account and the values shown in Fig. 5 are the average values where these are greater than 0.05 ppm. The figure demonstrates that the chemical shift contributions within helical regions seen in the alanine oligopeptide are reproduced in ribonuclease H.

The situation for β-sheets is more straightforward, in that the downfield shift observed experimentally is caused predominantly by the hydrogen-bonded carbonyl, as shown in Fig. 6b. The value of the downfield shift from the directly attached carbonyl group in a β-sheet structure tends to be slightly larger than that in an α-helix, reflecting a slightly shorter hydrogen-bonding distance compared to an α-helix (in ribonuclease H, average values are $d_N = 2.02$ Å for β-sheet and 2.10 Å for α-helix).

Thus, our calculations suggest that the main reason for the difference in NH chemical shifts in helices and sheets is not an effect from the directly hydrogen-bonded carbonyl, which is downfield in both cases, but the difference arises from an additional upfield shift predicted in helices and originating in residues i−2 and i−3. It is worth noting that the ring current shielding contributions to HN

chemical shifts in ribonuclease H are of similar magnitude to the bond magnetic anisotropy effects, making it difficult to characterise the magnetic anisotropy effects directly in the experimental data.

Distortions of peptide and protein helices

A strong periodicity of amide chemical shifts, and sometimes also of α-proton chemical shifts, is present in soluble amphipathic helices. Bruix et al. (1990) have observed a clear periodic variation of both amide and α-proton chemical shifts in a small synthetic peptide, Ac-(Leu-Lys-Lys-Leu)$_3$-NHEt, while studying a salt-induced coil-to-helix transition. Notable features of these profiles are the frequency of the variation, which matches the helix periodicity (3.6 residues per helix turn), and an apparent '180° phase shift' between amide and H^{α} profiles, i.e., minima in amide shifts matching maxima in H^{α} shifts. These findings were indicative of a relationship between secondary structure shifts and an intrinsic periodic property, alternating with the typical helix period. Periodic variations of secondary structure shifts have also been observed in several amphipathic peptides upon TFE-induced helix formation (Jiménez et al., 1992). In addition to amide and α-protons, β-protons sometimes display similar behavior in helical structures (Bruix et al., 1990; Kuntz et al., 1991; Blanco et al., 1992; Jiménez et al., 1992; Zhou et al., 1992).

Zhou et al. (1992) interpreted the periodicity of amide chemical shifts in terms of their dependency on hydrogen-bond length, short (i.e., strong) bonds leading to downfield shifts and long (i.e., weak) bonds leading to upfield shifts. Therefore, the phenomenon is considered to result from a shortening of hydrogen bonds on the hydrophobic side of helices and a lengthening of hydrogen bonds on the hydrophilic side. Because the hydrophobicity in helices is often periodic, the hydrogen-bond lengths, and hence the amide chemical shifts, would also be periodic.

Our calculations give similar results, although in our case the periodicity is not due to hydrogen bonding per se but to periodic variations in the N-H····O distance, which also provides an explanation for the observed periodicity in H^{α} shifts. The calculations therefore explain the periodicity, and can be used to investigate periodic effects in helices.

As an example of such periodic effects, we present calculations on the amide proton chemical shifts of the two-stranded α-helical coiled-coil GCN4 leucine zipper (Oas et al., 1990; O'Shea et al., 1991; Saudek et al., 1991), which clearly shows a regular experimental periodicity. The coordinates obtained from both X-ray diffraction at 1.8 Å resolution and NMR methods have been reported (PDB entries 2ZTA and 1ZTA, respectively). In the crystal structure, the individual α-helices are smoothly bent and the curvature is associated with shorter main-chain hydrogen bonds in the interface compared to the outside of the helices. There are two nonequivalent helices in the crystal structure, designated A and B, which give rise to substantially different calculated chemical shifts, as shown in Fig. 7. Neither molecule displays calculated shifts that agree well with the experimental values. This poor agreement most likely originates from differences between crystal and solution conformations, particularly since in solution only a single averaged signal is seen for each proton. Figure 8 shows a comparison of the experimental shifts with those calculated for the family of 20 NMR solution structures (Saudek et al., 1991) in which a marked

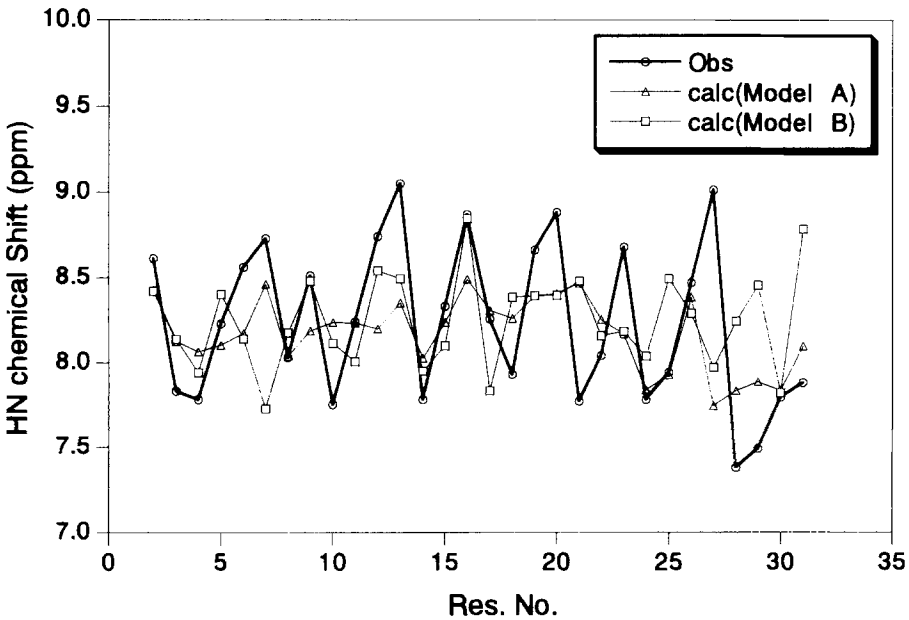

Fig. 7. Plot of sequence dependence of the calculated and observed amide proton shifts in GCN4 leucine zipper. The crystal structure is used, and the calculated values for the two independent molecules A and B are shown. ○: observed shifts; Δ: molecule A; □: molecule B.

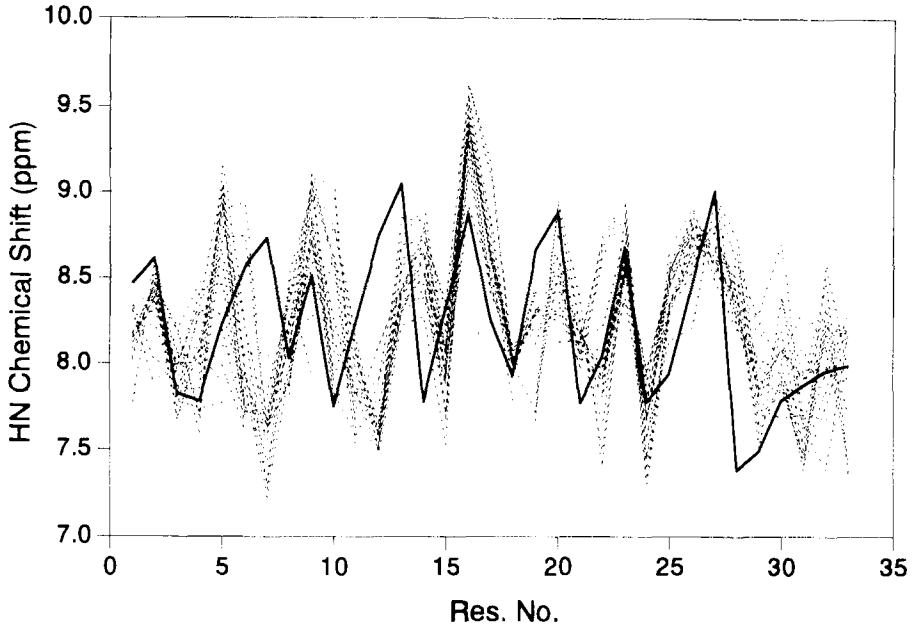

Fig. 8. Plot of sequence dependence of the calculated and observed amide proton shifts in GCN4 leucine zipper. The calculated values for the 20 NMR solution structures (Saudek et al., 1991) are shown. The coordinates were taken from PDB structure 1ZTA, and were calculated using distance geometry, followed by restrained energy minimization (DISMAN and GROMOS, respectively).

helix periodicity is predicted. The observed chemical shift value changes periodically along the peptide chain with a 3–4 residue repeat pattern, with seven maxima (i.e., large downfield shifts) at residues 7, 9, 13, 16, 20, 23, and 27, and eight minima at residues 4, 8, 10, 14, 18, 21, 24 and 28. The calculated shifts also have a 3–4 residue repeat pattern, with maxima at residues 5–6, 9–10, 13–14, 16, 20, 23, and 26–27 and minima at residues 3–4, 7, 11–12, 15, 18–19, 22, 24, 29 and 31–32. On comparing the calculated and experimental shifts, it can be seen that in general the agreement is extremely good between residues 15 and 28, but that after residue 28 there is virtually no agreement. However, both the calculated and experimental shifts agree in indicating a loss of periodicity at this point. The most interesting observation is that in the N-terminal half of the zipper, although both calculated and experimental shifts show clear periodicity, they are no longer in phase. This suggests that for the N-terminal half, in the true average solution structure the period of the helix coil is longer by roughly one residue compared to the NMR structures. Thus, calculations based on amide proton chemical shifts readily show a much closer resemblance of the NMR ensemble to the average solution structure compared to the crystal structure. However, the N-terminal half of the NMR ensemble is too tightly coiled.

Acknowledgements

This work was supported by the Japan Science Promotion Society as an International Cooperation between T.A. and M.P.W.

References

Abola, E., Bernstein, F.C., Bryant, S.H., Koetzle, T.F. and Weng, J. (1987) In *Crystallographic Databases – Information Content, Software Systems, Scientific Applications* (Eds, Allen, F.H., Bergerhoff, G. and Sievers, R.), Data Commission of the International Union of Crystallography, Bonn, pp. 107–132.

Adjadj, E., Mispelter, J., Quiniou, E., Dimicoli, J.L., Favoudon, V. and Lhoste, J.M. (1990) *Eur. J. Biochem.*, **190**, 263–271.

ApSimon, J.W., Craig, W.G., Demarco, P.V., Mathieson, D.W. and Saunders, L. (1967) *Tetrahedron*, **23**, 2357–2373.

Asakura, T., Ando, I. and Nishioka, A. (1977a) *Makromol. Chem.*, **178**, 1111–1132.

Asakura, T., Ando, I. and Nishioka, A. (1977b) *Makromol. Chem.*, **178**, 1521–1537.

Asakura, T. (1981) *Makromol. Chem.*, **182**, 1097–1109.

Asakura, T., Nakamura, E., Asakawa, H. and Demura, M. (1991) *J. Magn. Reson.*, **93**, 355–360.

Asakura, T., Niizawa, Y. and Williamson, M.P. (1992a) *J. Magn. Reson.*, **98**, 646–653.

Asakura, T., Demura, M., Nakamura, E. and Ando, I. (1992b) *Kobunshi Ronbunshu*, **49**, 281–287.

Bailey, S. (1994) *Acta Crystallogr.*, **D50**, 760–763.

Baker, E.N. and Hubbard, R.E. (1984) *Prog. Biophys. Mol. Biol.*, **44**, 97–179.

Bernstein, F.C., Koetzle, T.F., Williams, G.J.B., Meyer Jr., E.F., Brice, M.D., Rodgers, J.R., Kennard, O., Shimanouchi, T. and Tasumi, M. (1977) *J. Mol. Biol.*, **112**, 535–542.

Blanco, F.J., Herranz, J., González, C., Jiménez, M.A., Rico, M., Santoro, J. and Nieto, J.L. (1992) *J. Am. Chem. Soc.*, **114**, 9676–9677.

Bruix, M., Perello, M., Herranz, J., Rico, M. and Nieto, J.L. (1990) *Biochem. Biophys. Res. Commun.*, **167**, 1009–1014.

Bundi, A. and Wüthrich, K. (1979) *Biopolymers*, **18**, 299–311.

Case, D.A., Dyson, H.J. and Wright, P.E. (1994) *Methods Enzymol.*, **239**, 392–416.

Clayden, N.J. and Williams, R.J.P. (1982) *J. Magn. Reson.*, **49**, 383–396.

Dalgarno, D.C., Levine, B.A. and Williams, R.J.P. (1983) *Biosci. Rep.*, **3**, 443–452.

DiStefano, D.L. and Wand, A.J. (1987) *Biochemistry*, **26**, 7272–7281.

Eberle, W., Klaus, W., Cesareni, G., Sander, C. and Rösch, P. (1990) *Biochemistry*, **29**, 7402–7407.

Fairbrother, W.J., Palmer III, A.G., Rance, M., Reizer, J., Saier Jr., M.H. and Wright, P.E. (1992) *Biochemistry*, **31**, 4413–4425.

Haigh, C.W. and Mallion, R.B. (1980) *Progr. NMR Spectrosc.*, **13**, 303–344.

Heald, S.L., Tilton Jr., R.F., Hammond, L.J., Lee, A., Bayney, R.M., Kamarck, M.E., Ramabhadran, T.V., Dreyer, R.N., Davis, G., Unterbeck, A. and Tamburini, P.P. (1991) *Biochemistry*, **30**, 10467–10478.

Herranz, J., González, C., Rico, M., Nieto, J.L., Santoro, J., Jiménez, M.A., Bruix, M., Neira, J.L. and Blanco, F.J. (1992) *Magn. Reson. Chem.*, **30**, 1012–1018.

Jiménez, M.A., Blanco, F.J., Rico, M., Santoro, J., Herranz, J. and Nieto, J.L. (1992) *Eur. J. Biochem.*, **207**, 39–49.

Kabsch, W. and Sander, C. (1983) *Biopolymers*, **22**, 2577–2637.

Katayanagi, K., Minagawa, M., Matsushima, M., Ishikawa, M., Kanaya, S., Nakamura, H., Ikehara, M., Matsuzaki, T. and Morikawa, K. (1992) *J. Mol. Biol.*, **223**, 1029–1052.

Kikuchi, J., Fujita, K., Williamson, M.P. and Asakura, T. (1994) *Kobunshi Ronbunshu*, **51**, 409–413.

Kline, A.D. and Wüthrich, K. (1986) *J. Mol. Biol.*, **192**, 869–890.

Kuntz, I.D., Kosen, P.A. and Craig, E.C. (1991) *J. Am. Chem. Soc.*, **113**, 1406–1408.

Laskowski, R.A., MacArthur, M.W., Moss, D.S. and Thornton, J.M. (1993) *J. Appl. Crystallogr.*, **26**, 283–291.

Lee, B. and Richards, F.M. (1971) *J. Mol. Biol.*, **55**, 379–400.

Markley, J.L., Meadows, D.H. and Jardetzky, O. (1967) *J. Mol. Biol.*, **27**, 25–40.

McIntosh, L.P., Wand, A.J., Lowry, D.F., Redfield, A.G. and Dahlquist, F.W. (1990) *Biochemistry*, **29**, 6341–6362.

Oas, T.G., McIntosh, L.P., O'Shea, E.K., Dahlquist, F.W. and Kim, P.S. (1990) *Biochemistry*, **29**, 2891–2894.

Orban, J., Alexander, P. and Bryan, P. (1992) *Biochemistry*, **31**, 3604–3611.

Ösapay, K. and Case, D.A. (1991) *J. Am. Chem. Soc.*, **113**, 9436–9444.

Ösapay, K. and Case, D.A. (1994) *J. Biomol. NMR*, **4**, 215–230.

O'Shea, E.K., Klemm, J.D., Kim, P.S. and Alber, T. (1991) *Science*, **254**, 539–544.

Pelton, J.G., Torchia, D.A., Meadow, N.D., Wong, C.-Y. and Roseman, S. (1991) *Biochemistry*, **30**, 10043–10057.

Redfield, C. and Dobson, C.M. (1988) *Biochemistry*, **27**, 122–136.

Redfield, C. and Dobson, C.M. (1990) *Biochemistry*, **29**, 7201–7214.

Robertson, A.D., Purisima, E.O., Eastman, M.A. and Scheraga, H.A. (1989) *Biochemistry*, **28**, 5930–5938.

Saudek, V., Pastore, A., Morelli, M.A.C., Frank, R., Gausepohl, H. and Gibson, T. (1991) *Protein Eng.*, **4**, 519–529.

Szilágyi, L. (1995) *Prog. NMR Spectrosc.*, in press.

Szilágyi, L. and Jardetzky, O. (1989) *J. Magn. Reson.*, **83**, 441–449.

Wagner, G., Pardi, A. and Wüthrich, K. (1983) *J. Am. Chem. Soc.*, **105**, 5948–5949.

Wagner, G., Braun, W., Havel, T.F., Schaumann, T., Gō, N. and Wüthrich, K. (1987) *J. Mol. Biol.*, **196**, 611–639.

Williamson, M.P. (1990) *Biopolymers*, **29**, 1423–1431.

Williamson, M.P. and Asakura, T. (1991) *J. Magn. Reson.*, **94**, 557–562.

Williamson, M.P. and Asakura, T. (1992) *FEBS Lett.*, **302**, 185–188.

Williamson, M.P., Asakura, T., Nakamura, E. and Demura, M. (1992) *J. Biomol. NMR*, **2**, 83–98.

Williamson, M.P. and Asakura, T. (1993) *J. Magn. Reson. Ser. B*, **101**, 63–71.

Williamson, M.P., Kikuchi, J. and Asakura, T. (1995) *J. Mol. Biol.*, **247**, 541–546.

Wishart, D.S., Sykes, B.D. and Richards, F.M. (1991) *J. Mol. Biol.*, **222**, 311–333.

Wishart, D.S. and Sykes, B.D. (1994) *Methods Enzymol.*, **239**, 363–392.

Wishart, D.S., Bigam, C.G., Holm, A., Hodges, R.S. and Sykes, B.D. (1995) *J. Biomol. NMR*, **5**, 67–81.

Wüthrich, K. (1986) *NMR of Proteins and Nucleic Acids*, Wiley, New York, NY.

Xu, R.X., Nettesheim, D., Olejniczak, E.T., Meadows, R., Gemmecker, G. and Fesik, S.W. (1993) *Biopolymers*, **33**, 535–550.

Yamazaki, T., Yoshida, M. and Nagayama, K. (1993) *Biochemistry*, **32**, 5656–5669.

Zhou, N.E., Zhu, B.Y., Sykes, B.D. and Hodges, R.S. (1992) *J. Am. Chem. Soc.*, **114**, 4320–4326.

Zürcher, R.F. (1967) *Prog. NMR Spectrosc.*, **2**, 205–257.